Preprints of the 16th IFAC Symposium on System Identification
The International Federation of Automatic Control
Brussels, Belgium. July 11-13, 2012

Identification of the regional variability of the brain hemodynamic response to spontaneous and step-induced CO_2 changes using function expansions ⋆

Prokopis C. Prokopiou * **Kyle T.S. Pattinson** **
Richard G. Wise *** **Georgios D. Mitsis** *

* *Department of Electrical and Computer Engineering, University of Cyprus P.O. Box 20537, Nicosia 1678, Cyprus (e-mails: pproko01@ucy.ac.cy, gmitsis@ucy.ac.cy).*
** *Nuffield Department of Anaesthetics, University of Oxford John Radcliffe Hospital, Headington, Oxford OX3 9DU, UK (e-mail: kyle.pattinson@nda.ox.ac.uk)*
*** *School of Psychology, Cardiff University, UK (e-mail: wiserg@cardiff.ac.uk)*

Abstract:
The cerebrovascular bed is very sensitive to CO_2 changes, particularly in respiratory-related areas, such as the brainstem. Therefore, the hemodynamic response to such changes is of interest as it quantifies this sensitivity. Here, we examine in detail the regional characteristics of the hemodynamic response to spontaneous and larger, externally induced step CO_2 changes CO_2 (end-tidal forcing) by utilizing BOLD functional magnetic resonance imaging (fMRI) measurements from healthy humans. We first obtain estimates of the impulse response between CO_2 and BOLD signal in several anatomically and functionally defined regions of interest, using function expansions with different basis sets. These include the Laguerre basis, which has been widely used in linear and nonlinear systems identification particularly for biological/physiological systems, as well as different variants of gamma functions, which have been widely used in functional neuroimaging due to physiological considerations with regards to the characteristics of the BOLD response to external (sensory or other) stimuli. Based on the aforementioned comparisons, we perform the same analysis in smaller anatomical areas, considering voxel neighborhoods that span the entire image, in order to map key features of the hemodynamic response function such as peak value, time-to-peak and area, in finer spatial resolution.

1. INTRODUCTION

The cerebral vasculature is exquisitely sensitive to arterial CO_2 variations. This has been shown both using measurements of spontaneous cerebral blood flow velocity (CBFV) changes obtained with transcranial Doppler ultrasound (Mitsis et al. [2004]), as well as spontaneous variations in the blood oxygen level dependent (BOLD) signal obtained with functional magnetic resonance imaging (fMRI) (Wise et al. [2009]). Spontaneous end-tidal CO_2 variations were found to be correlated to low-frequency fluctuations of CBFV and the BOLD signal (Mitsis et al. [2004]-Wise et al. [2009]). In the latter study, significant regional variability in CO_2 sensitivity was revealed throughout the brain in a voxel-wise context, i.e. by correlating the signal in each voxel to the corresponding CO_2 changes. However, the waveform which quantifies the dynamic effects of CO_2 changes on the BOLD signal provides more information regarding the magnitude and timing of these effects, as well as their regional variability. These effects are particularly important in respiratory related areas in the brainstem and elsewhere, where CO_2 plays a major role (Feldman et al. [2003]). Here, we examine in detail the regional variability of the hemodynamic response function (HRF) to both spontaneous and larger externally induced CO_2 changes throughout the brain. In this context, we utilize function expansions and examine the effect of the choice of basis set on the obtained HRF estimates, initially using anatomical and functional (derived from the corresponding voxel-wise analysis) regions of interest (ROIs). Consequently, we examine smaller anatomical regions (voxel neighborhoods) in order to map the regional dependence of the CO_2 HRF waveform as well as the regional variability of its key features (e.g., peak value, time-to-peak, total area) in a finer spatial resolution.

2. METHODS

2.1 Experimental Methods

This is an extended analysis of the experimental data presented in Pattinson et al. [2009]. Twelve right-handed

⋆ Manuscript received April 11, 2012. This work was supported by the Medical Research Council (UK).

healthy volunteers, age 32 (SD(5)) yrs (3 female) participated in this study after giving written informed consent in accordance with the Oxfordshire Clinical Research Ethics Committee.

Respiratory protocols: The subjects wore a tight fitting facemask (Hans Rudolph, Kansas City, MO, USA) attached to a breathing system, which delivered mixtures of air, and CO_2. A minimum of ten minutes was allowed to adapt to the mask. Continuous recordings were made of end-tidal CO_2 and O_2, respiratory volume and oxygen saturations.

For the first half of the study (baseline resting breathing experiment) the subjects were asked to perform no particular task other than to remain awake. In the second half of the experiment, we delivered intermittent CO_2 challenges to stimulate breathing. The CO_2 challenges were delivered via a computer controlled gas mixing system (dynamic end-tidal forcing), (Robbins et al. [1982]). The CO_2 challenges were designed to raise the subjects P_{ETCO_2} by either 2 or 4 mmHg above a baseline level and lasted between 11 and 120 seconds (Fig. 1).

This methodology gave a good range of P_{ETCO_2} values for comparison with the resting-state data from the first half of the experiment. During this part of the experiment end-tidal oxygen (P_{ETO_2}) was maintained at 200mmHg, independent of changes in breathing, a value that is mildly above normal.

BOLD imaging: Two thousand seven hundred T2* weighted echo planar image (EPI) volumes were acquired on a Siemens Trio 3T scanner. The field of view (light gray shadow - Figure 2) comprised 16 coronal oblique slices of the brainstem (sequence parameters: TE=30 ms, TR=1 s, voxel size 2.5x2.5x3mm, flip angle 70^o). The experiment was divided into two stages, although scanning was continuous: The first 1130 images (18 minutes 50 seconds) comprised the baseline experiment and the final 1530 images (25 minutes 30 seconds) comprised the CO_2 stimulation experiment. The duration was determined by adaptation of a similar CO_2 challenge (Pedersen et al. [1999]) protocol for use in the MRI scanner. We also acquired a single volume whole head echo planar image taken with the same resolution and orientation as the brainstem scans to aid with registration to each subjects structural MRI scan and a high resolution T1 weighted structural scan (voxel size 1x1x1mm) to aid registration to common stereotactic space.

2.2 Mathematical Methods

Image preprocessing was carried out by using the Oxford Centre for Functional Magnetic Resonance Imaging of the Brain Software Library (FMRIB, Oxford, UK, FSL version 4.0). The following prestatistics processing were applied: removal of non brain structures (i.e. skull and surrounding tissues), spatial smoothing by using a Gaussian kernel of 5mm FWHM, mean-based intensity normalization of all volumes by the same factor, and high pass temporal filtering.

The brainstem is particularly susceptible to respiratory and cardiac noise. Therefore, in addition to standard

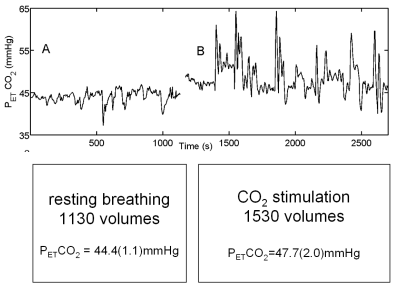

Fig. 1. Experimental protocol. The normal breathing protocol preceded the externally-induced CO_2 stimulation protocol (end-tidal forcing).

motion correction techniques, we also employed a modified version of noise correction technique, RETROICOR (Glover et al. [2000]) , in order to correct for cardiac and respiratory related noise. After preprocessing, the functional scans were registered to the MNI152 standard space using a linear registration method (FLIRTJenkinson et al. [1999]). Registration of the functional images to the T1 structural images was specifically optimized for the brainstem by using weighting masks that ensured accurate brainstem alignment. The voxel-wise time-series statistical analysis was carried out using FILM with local autocorrelation correction (Woolrich et al. [2001]), using P_{ETCO_2} as the regressor variable, and is described in more detail in (Pattinson et al. [2009]). For the first part of our analysis (ROIs) we used both anatomical and functional ROIs, the latter obtained from the voxels that exhibited significantly increased activation during CO_2 challenges at the group level.

Dynamic CO_2 reactivity was assessed by using linear (impulse response) and nonlinear (Volterra) models to quantify the relationship between P_{ETCO_2} and the averaged BOLD signal within each anatomically or functionally defined ROI. In this context, we employed the general Volterra model, which is given below for a Q-th order nonlinear system:

$$\begin{aligned} y(n) &= \sum_{q=0}^{Q} \sum_{m_1} ... \sum_{m_2} k_q(m_1, ..., m_q) x(n-m_1)...x(n-m_q) \\ &= k_0 + \sum_{m} k_1(m) x(n-m_1) + \\ &\sum_{m_1} \sum_{m_2} k_2(m_1 m_2) x(n-m_1) x(n-m_2) + ... \end{aligned} \quad (1)$$

where x(n) and y(n) are the system input and output respectively (i.e., P_{ETCO_2} and BOLD signal) and

$$k_q(m_1, ..., m_q)$$

are the Volterra kernels of the system, which describe the linear ($q = 1$) and nonlinear ($q > 1$) dynamic effects of the input on the output. The model of (1) reduces to the convolution sum for a linear system ($Q = 1$), with $k_1(m)$ corresponding to the impulse response of the system. Volterra models have been employed extensively for modeling physiological systems, since they are well-suited to the complexity of such systems (Marmarelis [2004]).

The impulse response or Volterra kernels can be estimated efficiently from input-output data, by utilizing function expansions in terms of an orthonormal basis (Marmarelis [2004]) :

$$k_q(m_1,...,m_q) = \sum_{j_1=0}^{L} ... \sum_{j_q=j_{q-1}}^{L} c_{j_1...j_q} b_{j_1}(m_1)...b_{j_q}(m_q) \quad (2)$$

where c_j are the expansion coefficients, $b_j(m)$ is the j-th order orthonormal basis function and $L+1$ is the total number of functions that yields an adequate system representation. By combining (1), (2) in matrix form:

$$\mathbf{y=Vc+e} \quad (3)$$

where the n-th row of $\mathbf{V}$ is given by [1, $v_1(n)$,..., $v_L(n)$, $(v_1(n))^2$, $v_1(n)v_2(n)$,...,$v_1(n)v_L(n)$,$(v_2(n))^2$,$v_2(n)v_3(n)$,..., $v_L(n)^2$] for a second-order system, ($Q=2$) with $v_j(n)$ denoting the convolution of the input with the j-th order orthonormal basis function. The expansion coefficients can then be obtained by the least-squares solution of (3):

$$c_{est} = [V^T V]^{-1} V^T y \quad (4)$$

The choice of basis set in the estimation of the CO_2 HRF is important, as it influences the obtained estimates. In this work, we used the Laguerre basis set, as well as alternative basis sets obtained from Gamma Probability Density functions (Hossein-Zadeha et al. [2003]), where singular value decomposition (SVD) was used to obtain the most significant components (singular vectors) from a set of gamma pdfs constructed by varying their shape and scale parameters. In the aforementioned study, motor task data (block design) and oddball task data (event-related) were used; hence, we consider a different range of parameters for the gamma functions to which we apply SVD as shown in (Fig. 2). The range of values that was considered was determined by the characteristics of the HRFs (time-to-peak, memory) obtained from the Laguerre basis.

After selecting the basis set for the data, our final purpose was to perform the analysis in smaller voxel neighbourhoods, where the signal to noise ratio (SNR) is considerably lower compared to larger ROIs. In order to improve the SNR, we used 3-D, 27-voxel masks around a central voxel (3x3x3 voxels) as shown in Fig. (3) and used the resulting weighted time-series to estimate the regionally-dependent HRF. The central voxel was weighted by 1 and all the remaining voxels by 0.0386. In this way, the central voxel was weighted more and the collective weight of all the remaining voxels was equal to the central voxel weight.

3. RESULTS

We present results obtained from linear models, whereby dynamic CO_2 reactivity is described by the system impulse response function, as nonlinear models were found to be only marginally better in terms of the achieved output prediction errors. The dynamic CO_2 reactivity waveforms for different anatonical and functional ROIs, using the Laguerre basis set, where shown in (Mitsis et al. [2008]) during spontaneous and forcing conditions. In Fig. (4) we show the dynamic reactivity waveforms of the same ROIs using the basis functions obtained after performing SVD

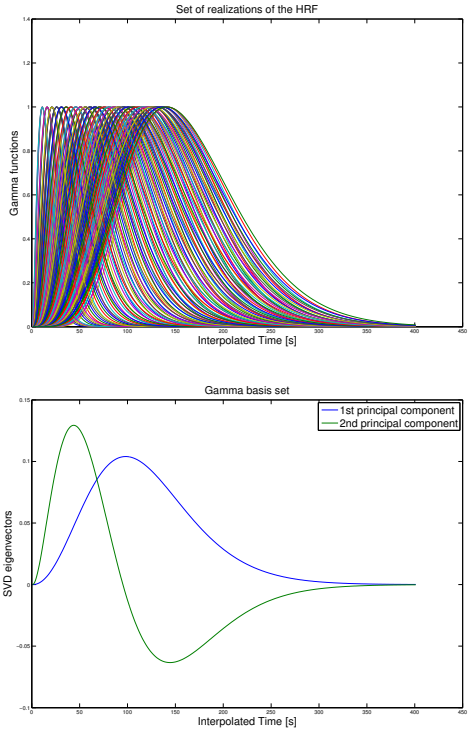

Fig. 2. (top panel) A set of 135 discrete samples taken at a rate of 10 samples/s (TR = 0.1 sec) from the Gamma model for the HRF. The location of the peak and the memory of each function were varied in accordance to the HRFs obtained from the Laguerre basis. (bottom panel) SVD analysis of the previous set of the HRF realizations revealed that the subspace formed by the first two eigenvectors is adequate for HRF estimation

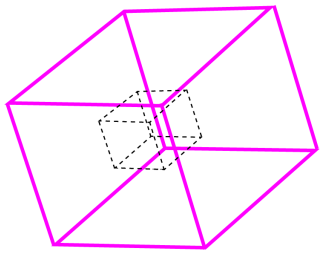

Fig. 3. Representation of the 3-D mask with the inner box (black dashed line) denoting the central voxel, which was weighted by 1. All the remaining voxels which lie in the space between the inner and the outer box were weighted by 0.0386 in order to yield a total weight equal to one

on the set of gamma functions, as described above. These waveforms quantify the dynamic effects of CO_2 on the BOLD signal, comfirming that a CO_2 increase results in a BOLD signal increase, with the maximum instantaneous effect occuring after around 4-8 sec.

We observe that the initial part of the waveforms suggest a similar dynamic response to spontaneous and larger CO_2 changes; however, the waveform obtained during resting conditions exhibited a late undershoot, which is absent

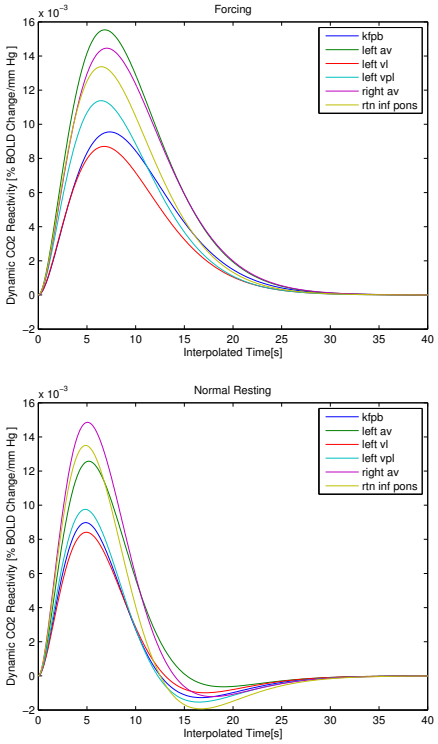

Fig. 4. Dynamic CO_2 reactivity in different ROIs during forcing (top panel) and resting (bottom panel) conditions, obtained using the Gamma pdf SVD analysis. The regional variability of CO_2 reactivity is evident. The undershoot observed during normal breathing is absent during forcing conditions. AV: anteroventral thalamus VL: ventrolateral thalamus, VRG: Ventral Respiratory Group, KFPB: Kolliker-Fuse parabrachial group, VPL: Ventral Posterior lateral thalamus, RTN: Retrotrapezoid nucleus.

from the forcing waveforms. This may be explained by the fact that the forcing condition happened with baseline hypercapnia, whereas the resting conditions did not.

Representative model predictions achieved by the Gamma and Laguerre basis function for the Left AV thalamus ROI are shown in (Fig. 5). The output prediction (BOLD signal) of both models is similar to each other.

As described above, we performed a similar analysis in smaller anatomical areas, considering voxel neighborhoods that span the entire image, in order to map key features of the hemodynamic response function in finer spatial resolution, using the 27 voxel mask to improve the SNR. We spanned the entire field of view by moving the central mask voxel in all directions and estimated the corresponding HRF during forcing and resting conditions. After the HRF was obtained, we assigned to the central voxel the HRF peak value, time-to-peak and total area, which reflect the characteristics of the hemodynamic response to CO_2 changes. A representative image of the peak values of the hemodynamic impulse response function in the entire image is ilustrated in (Fig. 6) for one subject both during forcing and resting conditions (top and bottom panels respectively). Similar maps were obtained for other subjects as well. The peak values are more pronounced during

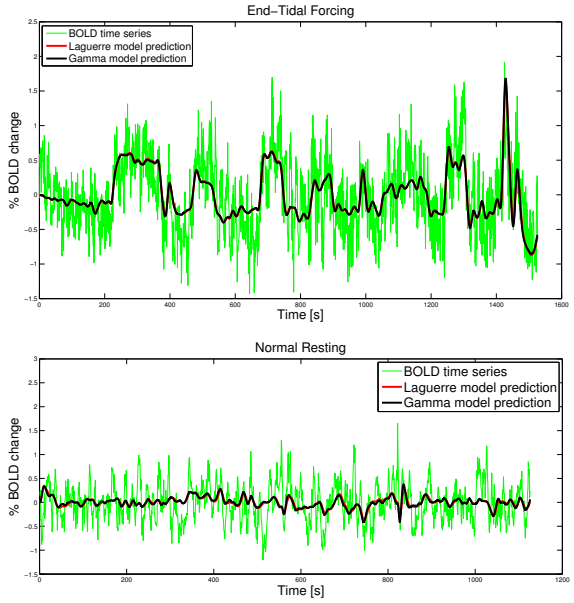

Fig. 5. Representative model output predictions for the AV Thalamus functional ROI during end-tidal forcing (top panel) and resting (bottom panel) conditions. We observe that the model prediction of both methods, Laguerre (red) and Gamma (black) are almost equal.

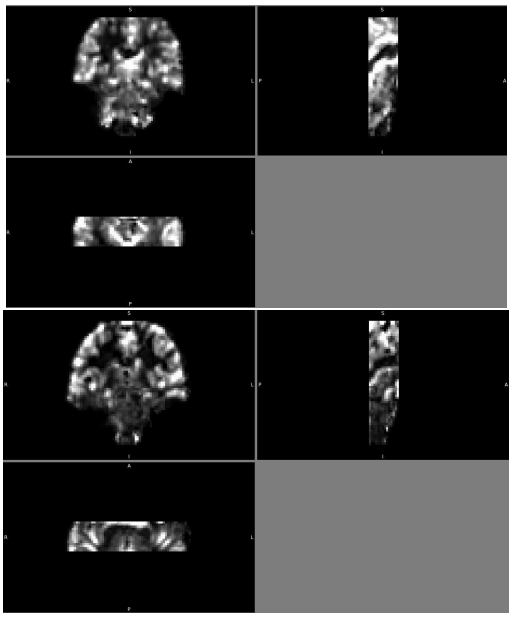

Fig. 6. Representative images of the peak values of the HRF corresponding to each image voxel. The top panel is the image obtained during forcing conditions and the bottom panel was obtained during resting conditions.)

forcing conditions compared to resting in areas such as the thalamus and brainstem.

The corresponding time-to-peak values are illustrated in Fig. (7). Darker values correspond to smaller time-to-peak values. Finally, in (Fig. 8) we illustrate the HRF area corresponding to each voxel. The map of the HRF area is similar to the peak value map shown in Fig. (6).

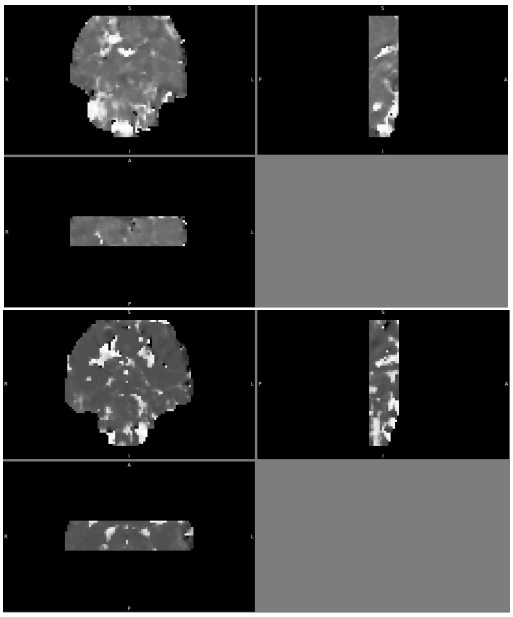

Fig. 7. Representative images of the time-to-peak values of the of the HRF corresponding to each image voxel. Top panel: forcing conditions, Bottom panel: resting conditions.

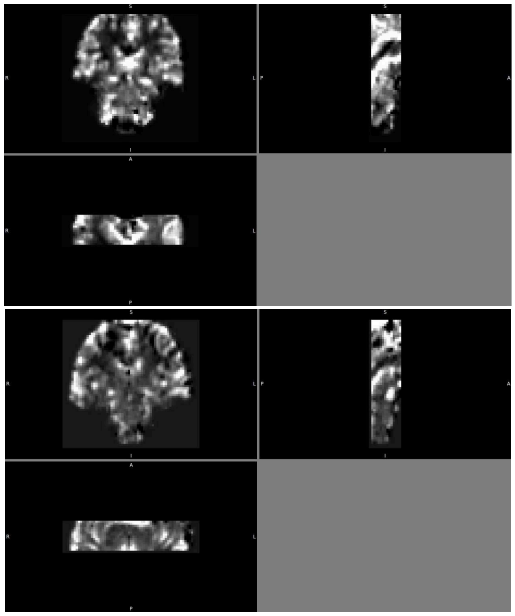

Fig. 8. Representative images of the area of the of the HRF corresponding to each image voxel. Top panel: forcing conditions, Bottom panel: resting conditions.

4. DISCUSSION AND CONCLUSIONS

In the present study, which is a further analysis of the experimental data described in (Pattinson et al. [2009]), we have rigorously examined the characteristics of the hemodynamic response to CO_2 changes (dynamic CO_2 reactivity) in brain regions that are implicated in respiratory control by utilizing BOLD fMRI measurements from healthy humans. To this end, we obtained HRF estimates for larger ROIs using function expansions in terms of the Laguerre basis and a basis set constructed from (physiologically motivated) Gamma pdfs using singular value decomposition, as well as for smaller voxel neighborhoods in order to obtain maps of the basic HRF characteristics in a fine spatial resolution. Since the SNR is lower in these smaller areas, we used 3-D masks to obtain weighted time-series. We performed this analysis for both basis sets; however, we present results from the SVD-derived Gamma pdf basis set which yielded less variable results overall, due to the low SNR. Note that the basic characteristics of the results obtained from the Laguerre basis in these smaller areas were generally similar.

The results show that there is considerable variability in the HRF characteristics. The results of the spatial maps for the HRF peak and are suggest that during resting conditions, reactivity to CO_2 is overall stronger in cortical areas compared to subcortical areas. However, during resting conditions, reactivity in cortical areas such as the thalamus and brainstem becomes more pronounced, which generally agrees with the voxel-wise results presented in (Pattinson et al. [2009]); however, note that in the latter study reactivity was assessed by a single coefficient in each voxel, using a general linear model. The time-to-peak maps are more uniform overall and suggest that cortical areas, as well as the thalamus and brainstem exhibit a faster response time to CO_2 changes.

The HRF maps from additional subjects exhibited similar patterns. We are currently working on obtaining average maps over the subject population in a standard space by registering the individual HRF maps to the standard Montreal Neurological Institute brain and aiming to compare the resulting average maps between the resting and forcing conditions.

REFERENCES

J.L. Feldman, G.S. Mitchell, and E.E. Nattie. Breathing: rhythmicity, plasticity, chemosensitivity. *Annu Rev Neurosci*, 21:239–66, 2003.

G.H. Glover, T.Q. Li, and D. Ress. Image-based method for retrospective correction of physiological motion effects in fMRI: RETROICOR. *Magn Reson Med*, 44: 162–7, 2000.

Gholam-Ali Hossein-Zadeha, Babak A. Ardekanib, and Hamid Soltanian-Zadeha. A signal subspace approach for modeling the hemodynamic response function in fMRI. *Magnetic Resonance Imaging*, 21:835–843, 2003.

M. Jenkinson, P. Bannister, M. Brady, and S. Smith. Improved optimization for the robust and accurate linear registration and motion correction of brain images. *Neuroimage*, 521 Pt 1:273–87, 1999.

V. Marmarelis. *Nonlinear Dynamic Modeling of Physiological Systems*. PiscatawayIEEE-Wiley, Piscataway NJ, 2004.

G.D. Mitsis, M.J. Poulin, Robbins P.A., and V.Z. Marmarelis. Nonlinear modeling of the dynamic effects of arterial pressure and CO2 variations on cerebral blood flow in healthy humans. *IEEE Trans. Biomed. Eng.*, 51(1):1932–1943, 2004.

G.D. Mitsis, A.K. Harvey, S. Dirckx, S.D. Mayhew, R. Rogers, I. Tracey, R.G. Wise, and K.T.S. Pattinson. Modeling of regional dynamic CO2 reactivity in respiratory related brain areas using BOLD fMRI. *Proc. 8th Intern. Conf. Bioinform. Bioengin. (BIBE)*, pages 1–5, 2008.

K.T.S. Pattinson, G.D. Mitsis, A.K. Harvey, S. Jhabdi, A.K. Dirckx, S. Mayhew, S.D.R. Rogers, I. Tracey, and R.G. Wise. Determination of the human brainstem respiratory control network and its cortical connections in vivo using functional and structural imaging. *Neuroimage*, 44:295–305, 2009.

M.E. Pedersen, M. Fatemian, and P.A. Robbins. Identification of fast and slow ventilatory responses to carbon dioxide under hypoxic and hyperoxic conditions in humans. *J Physiol*, 521 Pt 1:273–87, 1999.

P.A. Robbins, D.D. Swanson, and M.G. Howson. A prediction correction scheme for forcing alveolar gases along certain time courses. *J Appl Physiol*, 52:1353–7, 1982.

R.G. Wise, K. Ide, M.J. Poulin, and I. Tracey. Resting fluctuations in arterial carbon dioxide induce significant low frequency variations in BOLD signal. *Neuroimage*, 21:1652–64, 2009.

M.W. Woolrich, B.D. Ripley, M. Brady, and S.M. Smith. Temporal autocorrelation in univariate linear modeling of FMRI data. *Neuroimage*, 14:1370–86, 2001.